Zeszyty Naukowe Wydziału Elektroniki i Informatyki, Nr 4, pp. 29 – 42, 2012

Alexander Fedotov
Ivan Swito
Department of Energy Physics
Faculty of Physics
Belarusian State University
Minsk, Belarus

Yury Kalinin
Alexander Sitnikov
Department of Solid State Physics
Voronezh State Technical University
Voronezh, Russia

Aleksy Patryn
Katedra Podstaw Elektroniki
Wydział Elektroniki i Informatyki
Politechnika Koszalińska

DC conductivity mechanisms in granular nanocomposite films $Cu_x(SiO_2)_{1-x}$, deposited in Ar gas atmosphere

Keywords: DC conductivity, metal-insulator transition, nanocomposites, percolation

1. Introduction

Composite materials consisting of metallic or alloy ferromagnetic nanoparticles embedded into a dielectric matrix have occupied one of the center places in physics research at present time because of challenges thrown up by them both in theoretical understanding and practical applications [1]. One of reasons for this interest lies in the tendency to miniaturization and improvement of electronic magnetic devices performance and their aspiration to the field of higher frequencies [2]. The second reason is connected with the situation that up to now there is no complete understanding regarding the carrier transport mechanisms in many of metal-dielectric composites, when dimensions of metallic phase particles are approaching to nanometer scale. The third reason, that causes a large interest at present, is connected with the observed phenomena of the negative capacitance (inductive-like contribution into impedance) in some of nanocomposites and also possibilities to change their resistivity in wide region [3-5]. The last will allow to use such composites in future as electrotechnical elements with tunable resistance, capacitance and inductivity.

The character of DC/AC carrier transport in nanocomposites containing metallic nanoparticles randomly distributed in dielectric matrix should be strongly dependent on the composition of the material, and in particular, on the position of percolation threshold x_C. The latter is determined by atomic fraction of metallic phase x in composite, ratio of metallic and dielectric phases conductances σ_m/σ_d, phase composition of nanoparticles (the presence or lack of native oxides around them) and and matrix and also some geometric parameters of metallic phases (dimensions and their scattering, shape and topology of distribution of nanoparticles, etc.) [6-9]. In accordance with the percolation theory for binary composites [10], at $x < x_C$ continuous current-conducting (or percolating) cluster can not be formed, so that carrier transport is mainly realized by their tunneling from particle to particle through dielectric strata. However beyond the percolation threshold $x > x_C$, these particles can contact electrically to each other and therefore form continuous current-conducting clusters (or even their net when far beyond x_C) that will shunt dielectric phase shifting composite on metallic side of metal-insulator transition (MIT). Besides, for correct interpretation of the behavior of electric properties in many real composite materials we should also take into consideration the influence of the rest oxygen in a gas mixture at their preparation: the last can result in the formation of oxide "shells" or precipitates at the interface between metallic particles and dielectric matrix. All this makes the structure of such composites more complicated then for binary ones and can strongly change their properties.

As was shown earlier in our works [3,11] , in nanocomposite films containing FeCo-based nanoparticles embedded into dielectric matrix (alumina or PZT) maximal negative capacitance effect was observed when

nanocomposite is on dielectric side of MIT and its composition is close to the percolative configuration. Note that these effects were studied only for nanocomposites with magnetic metallic constituents (Fe, Co, Ni or their alloys) and never for the samples with non-magnetic highly-conductive metallic nanoparticles (like Cu or Al) in insulating matrix. So it was interesting to study electrical behavior of nanocomposites containing highly conductive nonmagnetic nanoparticles (like Cu) in dielectric matrixes compatible with silicon planar microelectronic technology (like SiO_2). Note that analysis of literature have shown only some papers concerning the study of electric properties in Cu-insulator nanocomposites [12-15].

So the goal of this work was to elucidate the influence of metal-to-dielectric component ration in the composite films, consisting of Cu-based nanoparticles embedded into dielectric (silica) matrix, on their structure and mechanisms of carrier transport basing on temperature dependences of DC conductivity.

2. Experimental procedures

The $Cu_x(SiO_2)_{1-x}$ thin film samples with $0.36 < x < 0.70$ in the range of 3 to 5 μm thick were fabricated by ion-beam sputtering of the compound target with argon onto the motionless glass ceramic substrate (5 cm ×25 cm). The deposition was carried out in a vacuum chamber (see, Fig. 1a) evacuate down to $1 \cdot 10^{-4}$ Pa and then filled with pure argon up to total gas pressure of $9.6 \cdot 10^{-2}$ Pa. The original configuration of the compound target (see, Fig. 1b) enabled the presented work to have composite films with different metallic to dielectric fraction ratio in one technological process [9, 16].

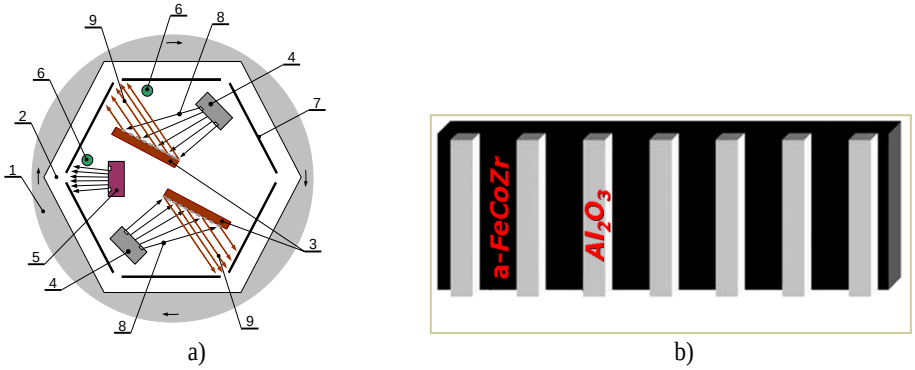

Fig. 1. The scheme of ion-beam sputtering set-up (a) and compound target (b) used for fabrication of nanocomposite filmes with the changing concentration of metallic phase. Sputtering deposition set-up (a): 1 – vacuum chamber; 2 – circling drum for substrates; 3 – sputtered targets; 4 – ion-beam source; 5 – source for ion-beam cleaning; 6 – compensators; 7 – dielectric substrates; 8 – ion beams; 9 – sputtered ions.

The as-deposited granular films were subjected to the study of structure by scanning electron microscopy (SEM) and X-ray diffraction (XRD). For XRD analysis Brucker powder diffractometer working with Cu K_α radiation, a graphite monochromator on the diffracted beam and a scintillation counter with pulse-height discriminator were used. Diffraction patterns were taken over a wide angular range from $2\theta = 5°$ to 80°. For SEM images the LEO 1455VP microscope was used. It was also equipped with a special microprobe X-Ray anslizer with energy-dispersive Si:Li detector Rontec allowing to perform X-Ray microanalysis for checking the samples` stoichiometry with accuracy of ~ 1%. Thicknesses of the films was also measured on SEM with accuracy ~ 2-3% on cleavages of the samples studied.

The nanocomposite films sputtered onto glass-ceramic substrates were cut into rectangular strips of 10 mm long and 2 mm wide samples. These samples were used for DC conductivity measurements at low electric field intensities $E < 10^5$ V/m when I-V characteristics were practrically linear. DC conductivity temperature dependences were measured in the temperature range 3 – 300 K using a closed-cycle cryogen-free cryostat system CFMS (Cryogenic Ltd., London), and PC based control system with Lakeshore Temperature Controller (Model 331), which allowed to scan the temperature with a rate of about 0.1-1 K/min and to stabilize it (if necessary) with accuracy 0.005 K. The relative error of conductance measurements was less than 0.1 %.

3. Structure characterization

SEM microscopy of the studied films with different concentration of metallic fraction is shown in Fig. 2. As is seen from images in Figs. 2a-2c, at $x < 0.60$ we observed their evolution from practically homogeneous to granular structure with x increase where the granules dimensions approached approximately 100 - 200 nm in the range of $0.50 < x < 0.58$.

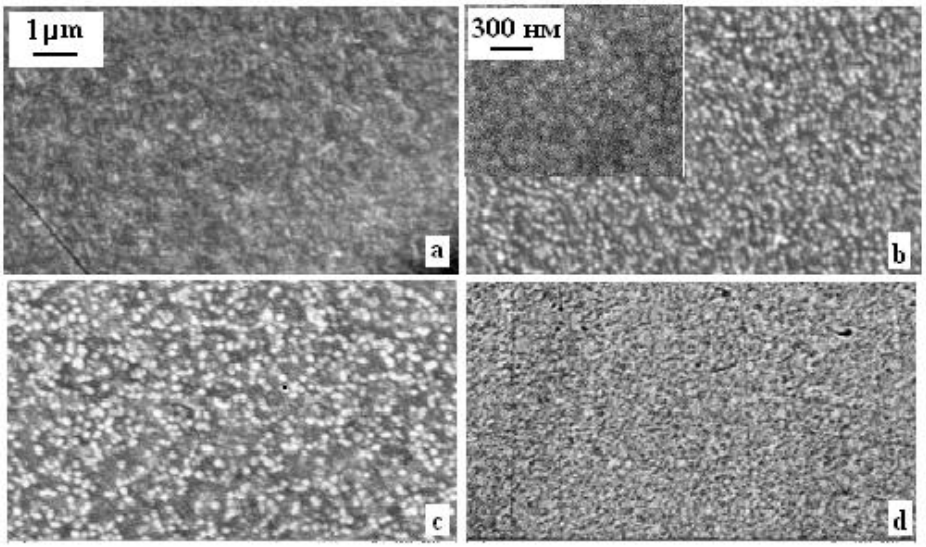

Fig. 2. SEM images of the surface of $Cu_x(SiO_2)_{1-x}$ films with x = 0.32 (a), 0.48 (b), 0.58 (c) and 0.69 (d). Light granules correspond to more high conductive phase. Insert in Fig. 2b corresponds to the film with x = 0.48 measured at 3 times greater magnification.

XRD in θ–2θ scan was used to characterize the structure of the films on a diffractometer D8 Advance Bruker AXS with a $Cu_{K\alpha}$ (with wavelength 0.15418 nm) radiation. Comparing XRD data for different samples we can drew some conclusions. Firstly, in our experiments X-ray diffraction patterns for the samples with small content x of Cu-based nanoparticles (less than 0.60) we observed strongly tailed diffraction lines

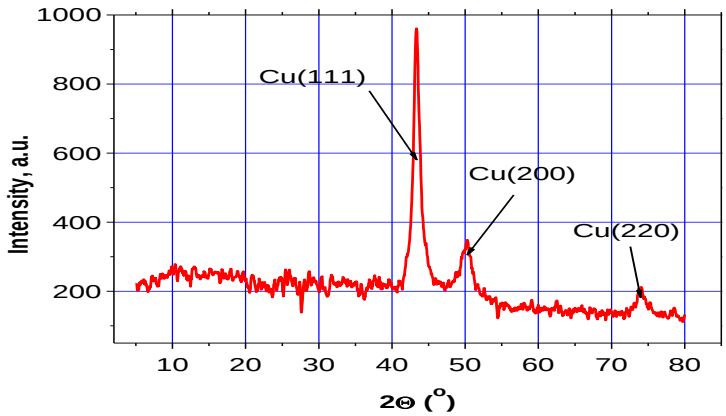

Fig. 3. X-ray diffraction pattern for the $Cu_x(SiO_2)_{1-x}$ film with x = 0.68.

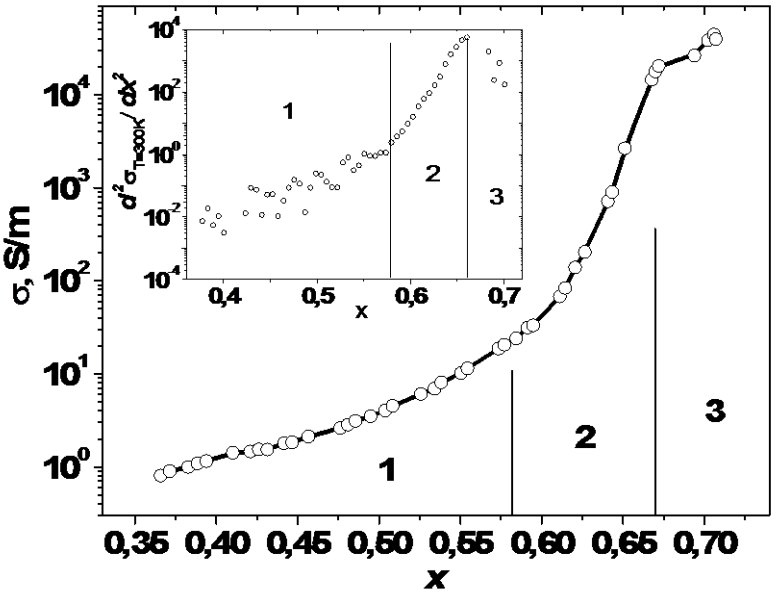

Fig. 4. Room temperature (300 K) conductivity σ vs atomic fraction x of Cu-based nanoparticles in the $Cu_x(SiO_2)_{1-x}$ film. Open circles are experimental points, continuous line is interpolating curve. Insert: Temperature dependences of second derivative of σ by x. Open circles are experimental points, continuous lines are interpolating curves.

which did not have clear peaks. Secondly, above this concentration of Cu-based fraction we observed 3 mostly pronounced diffraction lines (see, Fig. 3) in the range $40^o < 2\theta < 75^o$. Their positions allowed to attribute them, in accordance with the ASTM Charts, to metallic Cu. Note that we could not separate any extra CuO or CuO_2 lines. At the same time, as will be noted below, electric properties evidences possible limited oxidation of copper nanoparticles at least for $x < 0.6$ in the rest oxygen in vacuum chamber after its filling with Ar gas during deposition procedure.

4. DC conductivity

It is known that [2-10] composite properties are very sensitive to the position of percolation threshold x_C. So, the presented work studied the influence of composition on the position of percolation threshold and its influence on carrier transport mechanisms of the film nanocomposites.

The measured dependence of room temperature conductivity σ on concentration x of metallic fraction (Cu ions) in the studied films, shown in Fig. 4, display sigmoid-like behavior of $\sigma(x)$ curve which is characteristic for percolating systems. It is also seen that the increase of x in the studied range results in growth of conductivity on approx. 5 orders. However the character of $\sigma(x)$ curve have some peculiarities, one of which consists in that the mostly strong increase of σ with x (more than on 3 orders) occurs in the region 0.57 – 0.67 of x. In the clearest form, it is seen in insert in Fig. 4, where 2nd derivative of σ by x is presented (this was derived by graphical differentiation).

Comparison of the $\sigma'' = d^2\sigma/d\sigma^2$ dependence on x in Insert, derived by graphical differentiation of $\sigma(x)$ curve, and itself $\sigma(x)$ progress allows naturally to separate 3 characteristic parts of nanocomposites by metallic fraction concentration. As is seen, for region 1 we can see slow smooth increase of σ with x and nearly linear progress of $\sigma''(x)$ curve in Insert in Fig. 4. In the intermediate region 2 with 0.57 ат.% < x < 0.67 curve $\sigma(x)$ fits with the highest rate of σ growth with x and $\sigma''(x)$ has linear shape with more large slope than in region 1. Note also that this part 2 represents the range of compositions where composite samples had the pronounced granular-like SEM images (see, Fig. 2c). When x achieves the values of the order of 0.67, $\sigma(x)$ curve again goes to more slow increase (but σ'' falls down in Insert in Fig. 4). Note that just in this region 3 we observe again homogeneous SEM images for the samples (compare Fig. 2d and Fig. 4) and pronounced Cu peaks in XRD patterns (see, Fig. 3).

Analysis of temperature dependences of DC conductivity $\sigma(T)$, presented in Fig. 5, also shows their different behavior for the samples from the above mentioned 3 different regions of x values. As is seen from Fig. 5, all the samples studied can be divided on two parts by behavior of their $\sigma(T)$ curves. The samples from regions 1 and 2 in Fig. 4 displayed $\sigma(T)$ dependences with positive sign of ($d\sigma/dT$) values that is characteristic for thermally activated carrier transport on insulating side of MIT. In doing so, the samples of region 1 were characterized more sharp slopes in the low-temperature range (see, curves 1-3 in Fig. 5) whereas positive values of ($d\sigma/dT$) for the samples from region 2 was much less (curves 4 and 5).

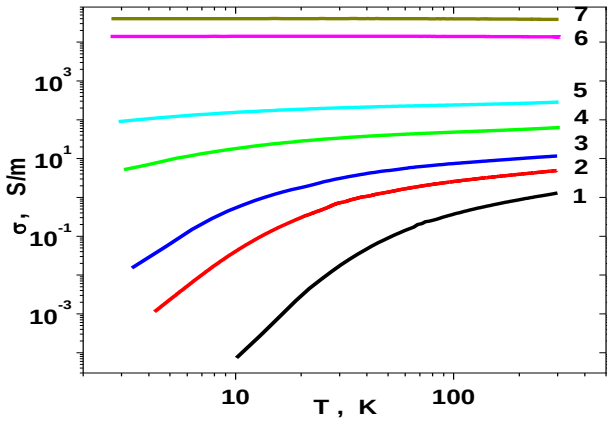

Fig. 5. Conductivity σ *vs* temperature T (in logarithmic scale) for $Cu_x(SiO_2)_{1-x}$ film nanocomposites with different content x of Cu ions in nanoparticles: 1- 0.397, 2 – 0.510, 3 – 0.558, 4 – 0.607, 5 – 0.628, 6 – 0.680 and 7 – 0.701.

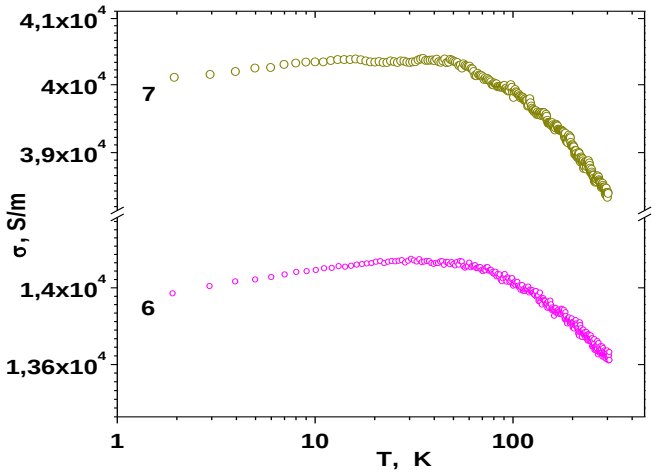

Fig. 6. Conductivity σ *vs* temperature T (in logarithmic scale) for $Cu_x(SiO_2)_{1-x}$ film nanocomposites with the same contents x of Cu ions in nanoparticles as for curves 6 and 7 in Fig. 5.

As follows from curves 6 and 7 with the lowest slopes in Fig. 5 for the films from region 3 in Fig. 4, they display positive values of ($d\sigma/dT$) only at low temperatures (below 30 K), see Fig. 6. At temperatures T > 40 K this curves are characterized by ($d\sigma/dT$) < 0 with power-like character of $\sigma(T)$ that is characteristic for metallic side of MIT.

5. Discussion

As was mentioned in Introduction, electric properties of nanocomposite materials are very sensitive to the position of the samples relative to the percolation threshold x_C. So, it was interesting to study the influence of composition and structure of the samples belonging to different regions 1-3 in Fig. 4 on carrier transport mechanisms of the $Cu_x(SiO_2)_{1-x}$ nanocomposites. In particular, we try to reveal the nature of transition of $\sigma(T)$ dependences from activational (with $(d\sigma/dT) > 0$) to power-like (with $(d\sigma/dT) < 0$) when x increasing.

As was mentioned in Section 4 above, for composite films belonging to the region 3 in Fig. 4 power-like $\sigma(T)$ dependence in Fig. 6, which is observed at temperatures over 30 K, indicates the metallic-like character of carrier transport. Taking into account transition from strong to weak values of $\sigma(x)$ slopes and change of $\sigma'(x)$ sign from positive to negative at crossing the boundary between regions 2 and 3 in Fig. 4, we can attribute such behavior of $\sigma(T)$ in region 3 by carrier transport along the percolating net of Cu nanoparticles which is fully completed in this region of x. On the other side, we can consider the boundary $x_{C0} \approx 0.57$-0.58 between regions 1 and 2, where the positive value of $\sigma'(x)$ is strongly changed (decreased), as the concentration where Cu nanoparticles begin to touch to each other and to form metallic highly-conducting net in the composite system $Cu_x(SiO_2)_{1-x}$. Note that this value x_{C0} is much higher than the percolation threshold x_C which should be close to 0.5 in accordance with 3D percolating model 10]. Although XRD patterns (see, Fig. 2) do not show features of the presence of Cu-based oxides in the studied $Cu_x(SiO_2)_{1-x}$ nanocomposites, we can suppose that the intrinsic percolation threshold is not realized due to partial oxidation of Cu nanoparticles by the rest oxygen in vacuum chamber filled with argon gas. For benefit of this assumption, as we believe, says the observed conservation of activational law of $\sigma(T)$ far beyond the x value of 0.50. In our opinion, this evidences that at $x < 0.57$-0.58 (boundary between regions 2 and 3) oxide "shells", which are mostly likelihood created around Cu nanoparticles, interlock the direct electrical contacts between Cu "cores" shifting the beginning of the Cu-"cores"-based percolating net formation to the x values close to 0.67-0.68. Beyond this concentration oxide "shells" becomes more spongiose due to deficiency of oxygen in vacuum chamber and can not totally prevent Cu-"cores" from their direct electric contact. Note that such behavior were observed in $FeCoZr$-Al_2O_3 and $FeCoZr$-$(PbZrTi)O_3$ composites [11,17] where metallic nanoparticles displayed "metallic core-oxide shell" nanostructure.

To understand the nature of activational law of $\sigma(T)$ dependences for the samples from regions 1 and 2 (insulating side of MIT) in Fig. 4, we re-plotted curves $\sigma(T)$ in Arhenius scale. The rescaled curves in Fig. 7 are characterized by changing ("sliding") energies of activation which are decreased with temperature lowering. Such behavior confirms predomination of the mentioned above thermally activated tunneling of carriers over Cu nanoparticles in Variable Range Hopping (VRH) regime. As is known,

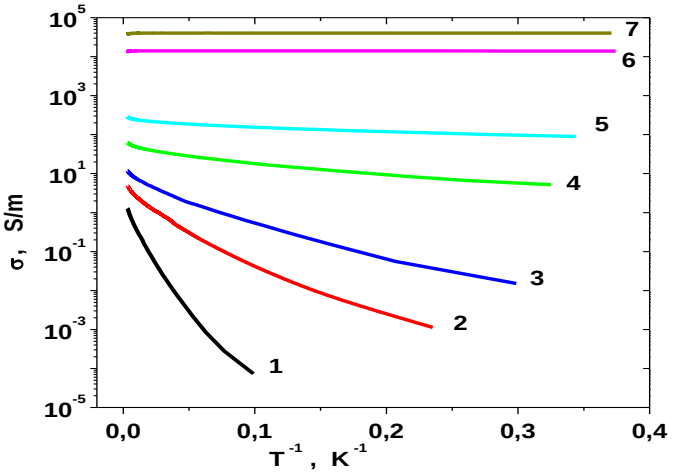

Fig. 7. Conductivity σ *vs* temperature T (in Arhenius scale) for $Cu_x(SiO_2)_{1-x}$ film nanocomposites with different content x of Cu ions in nanoparticles: 1- 0.397, 2 – 0.510, 3 – 0.558, 4 – 0.607, 5 – 0.628, 6 – 0.680 and 7 – 0.701

temperature dependences of conductivity in hopping regime is usually described by the known relation [18]

$$\sigma(T) = \sigma_0 \exp [- (T_0/T)]^{\lambda},$$

where σ_O and T_O are constants characterizing the material, and the exponent λ depends on particular VRH type. To reveal the likely type of VRH mechanism we presented $\sigma(T)$ for 3 mostly characteristic samples from dielectric side of MIT (regions 1 and 2) in Mott scale with two different exponent λ values equaled by 0.25 and 0.5 (see, Fig. 8). These dependences were imaged for comfort of presentation in the normalized form $\ln(\sigma/\sigma_{300}) \propto -(T_O/T)^{\lambda}$ due to strong difference in conductivities of the samples studied. Analysis of dependences, observed in Fig. 8, shows that for all studied samples of groups 1 and 2 linearisation of these curves is satisfied for λ = 0.5 in the mostly wide range of temperatures (see, Fig. 8a). This means that in the studied samples the observed VRH

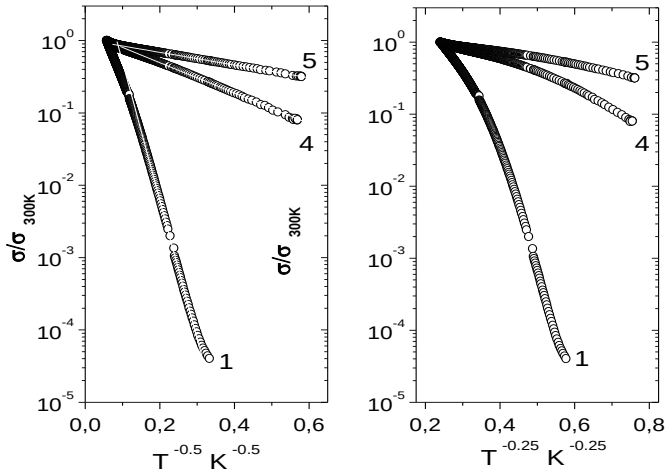

Fig. 8. Normalized conductivity (σ/σ_{300}) *vs* temperature *T* in Mott scale for $Cu_x(SiO_2)_{1-x}$ film nanocomposites with the same contents *x* of Cu ions in nanoparticles as for curves 1, 4 and 5 in Fig. 5.

mechanism corresponds with the known Shklovski-Efros model [19] which describes carrier hopping at the presence of Coulomb gap in density of localized states around Fermi level. The latter evidences that in the studied nanocomposites, being on insulating side of MIT, carrier transport is realized by jumps of electrons over the localized states in silica between Cu nanoparticles with "core-shell" nanostructure.

Resume

The presented work revealed that concentration of Cu fraction in $Cu_x(SiO_2)_{1-x}$ nanocomposites manufactured by ion-beam sputtering in Ar gas atmosphere have a very strong influence on structure (studied by SEM and XRD) and carrier transport (DC conductivity) of films containing Cu-based nanoparticles embedded into amorphous silica matrix.

1. SEM measurements evidences that the films shows apparent features of the formation of nanogranular structure at $0.45 < x < 0.60$ as compared to the samples with $x < 0.45$ or $x > 0.58$. for the samples deposited in pure Ar.
2. Composite films with $x < 0.68$ are on dielectric side of MIT and possess thermally activated carrier transport whereas the samples belonging to $x > 0.68$ indicate the metallic-like character of conductance along the percolating net of Cu nanoparticles inside of silica matrix.
3. In nanocomposites with $x < 0.68$ where dielectric regime of DC carrier transport is realized VRH mechanism described by Shklowski-Efros law is observed.

Acknowledgements

The authors would like to acknowledge the financial support from VISBY Program of the Swedish Institute.

Bibliography

1. Y. Imry. *Nanostructures and Mesoscopic Systems*, edited by W. P. Kirk and M. A. Reed (Academic, New York, 1992).
2. *Nanotechnology*, edited by G. Timp (Springer, New York, 1999).
3. P. Zhukowski, T.N. Kołtunowicz, P. Wegierek, J.A. Fedotova, A.K. Fedotov and A.V. Larkin. *Formation of Noncoil-Like Inductance in Nanocomposites* $(Fe_{0.45}Co_{0,45}Zr_{0,10})_x(Al_2O_3)_{1-x}$ *Manufactured by Ion-Beam Sputtering of Complex Targets in* $Ar+O_2$ *Atmosphere*. Acta Physica Polonica. 120 (1), pp. 43-45. 2011.
4. A.M. Saad, A.K. Fedotov, J.A. Fedotova, I.A. Svito, B.V. Andrievsky, Yu.E. Kalinin, V.V. Fedotova, V. Malyutina-Bronskaya, A.A. Patryn, A.V. Mazanik, and A.V. Sitnikov. *Characterization of* $(Co0.45Fe0.45Zr0.10)_x(Al2O3)_{1–x}$ *nanocomposite films applicable as spintronic materials*. Phys. stat. sol. (c) 3 (5), pp. 1283–1290. 2006.
5. A.M. Saad, A.V. Mazanik, Yu.E. Kalinin, J.A. Fedotova, A.K. Fedotov, S. Wrotek, A.V. Sitnikov and I.A. *Svito. AC and DC carrier transport in* $(FeCoZr)_x(Al_2O_3)_{1-x}$ *nanocomposite films for spintronic applications*. SEMINANO 2005, Budapest, Hungary, September 10-12, pp. 321-324. 2005.
6. R. Wood. *Feasibility of Magnetic Recording at 1 Terabit per Square Inch*. IEEE Trans. Magn. 36, pp. 36–42. 2000.
7. C. Baker, S. K. Hasanain, S. Ismat Shaha. *The magnetic behavior of iron oxide passivated iron nanoparticles.* J. Appl. Phys. 96 (11) pp. 6657-6662. 2004.
8. Xianghui Huang and Zhenhua Chen. *Preparation of CoFe2O4/SiO2 nanocomposites by sol–gel method*. Journal of Crystal Growth, 271(1-2), pp.287-293. 2004.
9. Yu.E. Kalinin, A.N. Remizov, and A.V. Sitnikov. *Electric propertries of amorphous nanocomposites* $(Co_{45}Fe_{45}Zr_{10})_x(Al_2O_3)_{100-X}$. Bulletin of Voronezh State Technical University: Material Science, N113, pp. 43-49. 2003.
10. Grimmet G. *Percolation*. (Berlin: Springer-Verlag, 2nd ed., 1999).
11. J. V. Kasiuk, J. A. Fedotova, M. Marszalek, A. Karczmarska, M. Mitura-Nowak, Yu. E. Kalininc, and A. V. Sitnikov. *Effect of Oxygen Pressure on Phase Composition and Magnetic Structure of* $FeCoZr–Pb(ZrTi)O_3$ *Nanocomposites*. Physics of the Solid State 54 (1), pp. 178–184. 2012.
12. W. Chen, J. J. Lin, X. X. Zhang, H. K. Shin, J. S. Dyck et al. *Electrical conductivity and thermopower of* $Cu–SiO_2$ *nanogranular films*. Appl. Phys. Letters 81 (3), pp. 523-525. 2002
13. X. X. Zhang, Chuncheng Wan, H. Liu, Z. Q. Li, and Ping Sheng J. J. Lin. *Giant Hall Effect in Nonmagnetic Granular Metal Films*. Phys. Ren. Letters 86 (24), pp. 5562-5565. 2001.
14. I.D. Kosobudski, A.S. Dzhumaliev, K.V. Zapsis, N.M.Ushakov. *Copper-containing nanocomposites. Synthesis and the composition study.* Letters to J. of Thechn. Physics. 30 (11), pp. 94-98. 2004.
15. S. Banerjee and D. Chakravorty. *Electrical resistivity of copper-silica nanocomposites synthesized by electrodeposition.* J. Appl. Phys. **84**, pp. 1149-1151. 1998.
16. A.M. Saad, A.V. Mazanik, Yu.E. Kalinin, J.A. Fedotova, A.K. Fedotov, S. Wrotek, A.V. Sitnikov and I.A. Svito *Structure and electrical properties of CoFeZr-aluminium oxide nanocomposite films*. Reviews on Advanced Materials Science 8, pp. 152-157. 2004.
17. J. Fedotova , J. Przewoznik, C. Kapusta, M. Milosavljević, J.V. Kasiuk, P. Zukrowski, M. Sikora, A.A. Maximenko, D. Szepietowska, K.P. Homewood. *Magnetoresistance in* $FeCoZr\text{-}Al_2O_3$ *nanocomposite films containing "metal core-oxide shell" nanogranules.* J. Phys. D. 44, pp.1-12. 2011
18. N.F. Mott and E.A. Devis. *Electron processes in noncrystalline materials* (Clarendon Press, Oxford,1979).
19. Efros A.L., Shklovski B.V. *Critical behaviour of conductivity and dielectric constant near the metal-nonmetal transition threshold*. Phys. Stat. Sol. (b) 76(2), pp. 475-485. 1986

Abstract

In the article are presented the results of the study of structure of $Cu_x(SiO_2)_{1-x}$ nanocomposites with a wide range of metallic fraction content and their DC conductivity measured in the temperature range between 3 and 300 K.

The $Cu_x(SiO_2)_{1-x}$ thin film samples with $0.36 < x < 0$ and thicknesses 3 to 5 μm were fabricated by ion-beam sputtering of the compound Cu/SiO_2 target with argon onto the glass ceramic substrate.

The as-deposited films displayed their evolution from practically homogeneous (at $x < 0.50$) to granular (in the range of $0.50 < x < 0.58$) structure with x increase where the granules dimensions approached approximately 100 - 200 nm.

The study of conductivity have shown that the studied nanocomposite films with $x < 0.68$ are on dielectric side of metal-insulator transition and possess thermally activated tunneling of electrons between Cu nanoparticles whereas the samples with $x > 0.68$ indicate the metallic-like character of conductance along the percolating net of Cu nanoparticles inside of silica matrix.

In dielectric regime (for nanocomposites with $x < 0.68$) DC carrier transport is realized by VRH mechanism described by Shklowski-Efros law, by jumps of electrons between Cu nanoparticles.

Streszczenie

W artykule przedstawiono rezultaty badań struktury nanokompozytów $Cu_x(SiO_2)_{1-x}$ w szerokim zakresie zawarcia fazy metalicznej and ich DC przewodnictwo zmierzone w zakresie temperatur od 3 do 300K. Cienkie warstwy $Cu_x(SiO_2)_{1-x}$ z $0.36 < x < 0$ i grubością 3 I 5 μm były przygotowane poprzez rozpylanie wiązką argonową jonową kompaunda Cu/SiO_2 tarczy na podłoże ze szklanej ceramiki. Wszystkie warstwy po napylaniu wykazywały transformację struktury od praktycznie jednorodnej (dla $x < 0.50$) do granulowanej ($0.50 < x < 0.58$) gdzie, ze wzrostem x liniowe rozmiary granul osiągają 100-200 nm.

Badania przewodnictwa wykazało że nanokompozytowe filmy z $x < 0.68$ są po dielektrynej stronie przejścia metal-izolator i wykazują termiczne aktywowane tunelowanie elektronów pomiędzy Cu nanocząstkami, w tym czasie jak przy $x > 0.68$ zauważono przewodność podobną do metalicznej wzdłuż perkolacyjnej sieci nanocząstek Cu wewnątrz matrycy silicydu.

W trybie dielektrycznym (dla nanocząstek z $x<0.68$) transport nośników jest realizowany wg VRH mechanizmu zgodnie z prawem Shklowskiego-Efrosa, poprzez skoki elektronów pomiędzy Cu nanocząstkami.